

Comparing Different Deep Learning Architectures for Classification of Chest Radiographs

Keno K. Bressem, Lisa Adams, Christoph Erxleben, Bernd Hamm, Stefan Niehues, Janis Vahldiek

Department of Radiology, Charité Universitätsmedizin Berlin

`keno-kyrill.bressem(at)charite.de`

Abstract

Chest radiographs are among the most frequently acquired images in radiology and are often the subject of computer vision research. However, most of the models used to classify chest radiographs are derived from openly available deep neural networks, trained on large image-datasets. These datasets routinely differ from chest radiographs in that they are mostly color images and contain several possible image classes, while radiographs are greyscale images and often only contain fewer image classes. Therefore, very deep neural networks, which can represent more complex relationships in image-features, might not be required for the comparatively simpler task of classifying grayscale chest radiographs. We compared fifteen different architectures of artificial neural networks regarding training-time and performance on the openly available CheXpert dataset to identify the most suitable models for deep learning tasks on chest radiographs. We could show, that smaller networks such as ResNet-34, AlexNet or VGG-16 have the potential to classify chest radiographs as precisely as deeper neural networks such as DenseNet-201 or ResNet-151, while being less computationally demanding.

Introduction

Chest radiographs are among the most frequently used imaging procedures in radiology. They have been widely employed in the field of computer vision, as chest radiographs are a standardized technique and, if compared to other radiological examinations such as computed tomography or magnetic resonance imaging, contain a smaller group of relevant pathologies. Although many artificial neural networks for the classification of chest radiographs have been developed, it is still the subject of intensive research. Only a few groups design their own networks from scratch, but rather use already established architectures, such as ResNet-50 or DenseNet-121 (with 50 and 121 representing the number of layers within the respective neural network) [3][5][7][2][14][11]. These neural networks have often been trained on large, openly available datasets, such as ImageNet, and are therefore already able to recognize numerous image features. When training a model for a new task, such as the classification of chest radiographs, the use of pre-trained networks may improve the training speed and accuracy of the new model, since important image features that have already been learned can be transferred to the new task and do not have to be learned again. However, the feature space of freely available data sets such as ImageNet differs from chest radiographs as they contain color images and more categories. The ImageNet Challenge includes 1000 possible categories per image, while CheXpert, a large freely available data set of chest radiographs, only distinguishes between 14 categories (or classes)[13]. Although the ImageNet challenge showed a trend towards higher accuracies for deeper networks, this may not be fully transferrable to radiology. In radiology, sometimes only limited features of an image can be decisive for the diagnosis. Therefore, images cannot be scaled down as much as desired, as the required information would otherwise be lost. But, the more complex a neural network architecture is, the more resources are required for training and deployment of such an algorithm. As up-scaling the input-images resolution exponentially increases memory usage during training for large neural networks, that evaluate many parameters, the size of a mini batch needs to be reduced earlier and more strongly, potentially affecting optimizers such as stochastic gradient descent. Therefore, it is currently not clear, which of the available artificial neural networks designed for and trained on the ImageNet dataset will perform the best for the classification of chest radiographs. The hypothesis of this work is, that shallow networks are already sufficient for the classification of radiographs

and might even outperform deeper networks while requiring lesser resources. Therefore, we systematically examine the performance of fifteen openly available artificial neural network architectures in order to identify the most suitable ones for the basic classification of chest radiographs.

Methods

Data preparation

The free available CheXpert dataset consists of 224,316 chest radiographs from 65,240 patients. Fourteen findings have been annotated for each image: enlarged cardiomeastinum, cardiomegaly, lung opacity, lung lesion, edema, consolidation, pneumonia, atelectasis, pneumothorax, pleural effusion, pleural other, fracture and support devices. Hereby the findings can be annotated as present (1), absent (NA) or uncertain (-1). Similar to previous work on the classification of the CheXpert dataset [7][16], we trained these networks on a subset of labels: cardiomegaly, edema, consolidation, atelectasis and pleural effusion. As we only aim at network comparison and not on maximal precision of a neural network, for this analysis, each image with an uncertainty label was excluded, other approaches such as zero imputation or self-training were also not adopted. Furthermore, only frontal radiographs were used, leaving 135,494 images from 53,388 patients for training. CheXpert offers additional dataset with 235 images (201 images after excluding uncertainty labels and lateral radiographs), annotated by two independent radiologists, which is intended as an evaluations dataset and was therefore used for this purpose.

Data augmentation

For the first and second training session, the images were scaled to 320 x 320 pixels, using bilinear interpolation, and pixel values were normalized. During training, multiple image-transformations were applied: flipping of the images alongside the horizontal and vertical axis, rotation of up to 10°, zooming of up to 110%, adding of random lightning or symmetric wrapping.

Model training

14 different convolutional neural networks (CNN) of five different architectures (ResNet, DenseNet, VGG, SqueezeNet and AlexNet) were trained on the CheXpert dataset [3][5][17][6][9]. All training was done using the Python programming language (<https://www.python.org>, version 3.8) with the PyTorch (<https://pytorch.org>) and FastAI (<https://fast.ai>) libraries on a workstation running on Ubuntu 18.04 with two Nvidia GeForce RTX 2080ti graphic cards (11 GB of RAM each)[4][10]. In the first training session, batch size was held constant at 16 for all models, while it was increased to 32 for all networks in the second session. In the first two sessions, each model was trained for eight epochs, whereas during the first five epochs only the classification-head of each network was trained. Thereafter, the model was unfrozen and trained as whole for three additional epochs. Before training and after the first five epochs, the optimal learning rate was determined [19], which was between 1e-1 and 1e-2 for the first five epochs and between 1e-5 and 1e-6 for the rest of the training. We trained one multilabel classification head for each model. Since the performance of a neural network can be subject to minor random fluctuations, the training was repeated for a total of five times. The predictions on the validation data set were then exported as comma separated values (CSV) for evaluation.

Evaluation

Evaluation was performed using the “R” statistical environment including the “tidyverse” and “ROCR” libraries [12][20][18]. Predictions on the validation dataset of the five models for each network architecture were pooled so that the models could be evaluated as a consortium. For each individual prediction as well as the pooled predictions, receiver operation characteristic (ROC) curves and precision recall curves (PRC) were plotted and the areas under each curve were calculated (AUROC and AUPRC). AUROC and AUPRC were chosen as they enable a comparison of different models, independent of a chosen threshold for the classification.

Results

The CheXpert validation dataset consists out of 234 studies of 200 patients, not used for training with no uncertainty-labels. After excluding lateral radiographs (n = 32), 202 images of 200 patients remained.

The dataset presents class imbalances (% positives for each finding: cardiomegaly 33%, edema 21%, consolidation 16%, atelectasis 37%, pleural effusion 32%), so that the AUPRC as well as the AUROC can be considered equally important measurements for the performance of the network. The performance of the tested networks is compared to the AUROC reported by Irvin et al.[7]. However, only values for AUROC, but not for AUPRC, are provided there. In most cases, the best results were achieved with a batch size of 32, so all the information provided below refers to models trained with this batch size. Results achieved with smaller batch sizes of 16 will be explicitly mentioned.

Area under the Receiver Operating Characteristic Curve

Deeper artificial neural networks generally achieved higher AUROC values than shallow networks (Table 1 and Figures 1-3). Regarding the pooled AUROC for the detection of the five pathologies, ResNet-152 (0.882), DenseNet-161 (0.881) and ResNet-50 (0.881) performed best (Irvin et al. CheXpert baseline 0.889)[7]. Broken down for individual findings, the most accurate detection of atelectasis was achieved by ResNet-18 (0.816, batch size 16), ResNet-101 (0.813, batch size 16), VGG-19 (0.813, batch size 16) and ResNet-50 (0.811). For detection of cardiomegaly, the best four models surpassed the CheXpert baseline of 0.828 (ResNet-34 0.840, ResNet-152 0.836, DenseNet-161 0.834, ResNet-50 0.832). For congestion, the highest AUROC was achieved using ResNet-152 (0.917), ResNet-50 (0.916) and DenseNet-161 (0.913). Pulmonary edema was most accurately detected using DenseNet-161 (0.923), DenseNet-169 (0.922) and DenseNet-201 (0.922). For pleural effusion, the four best models were ResNet-152 (0.937), ResNet-101 (0.936), ResNet-50 (0.934) and DenseNet-169 (0.934), all of which performed superior to the CheXpert baseline of 0.928.

Area under the Precision Recall Curve

For AUPRC, shallower artificial neural networks could achieve higher values than deeper network-architectures (Table 2 and Figures 4-6). The highest pooled values for the AUPRC were achieved by training VGG-16 (0.709), AlexNet (0.701) and ResNet-34 (0.688). For atelectasis, CGG-16 and AlexNet both achieved the highest AUPRC of 0.732, followed by Resnet-35 with 0.652. Cardiomegaly was most accurately detected by SqueezeNet 1.0 (0.565),

Alexnet-152 (0.565) and Vgg-13 (0.563). SqueezeNet 1.0 also achieved the highest AUPRC values for consolidation (0.815) followed by ResNet-152 (0.810) and ResNet-50 (0.809). The best classifications of pulmonary edema were achieved by DenseNet-169, DenseNet-161 (both 0.743) and DenseNet-201 (0.742). Finally, for pleural effusion ResNet-101 and ResNet-152 achieved the highest AUPRC of 0.591, followed by ResNet-50 (0.590).

Overall best Performance

Considering both AUROC and AUPRC, the best performance was achieved by VGG-16 (AUROC: 0.856, AUPRC: 0.709), ResNet-34 (AUROC: 0.872, AUPRC: 0.688) and AlexNet (AUROC: 0.839, AUPRC: 0.701), all with a batch size of 32.

Training time

Fourteen different network-architectures were trained 10 times each with a multilabel-classification head (five times each for batch size of 16 or 32 and an input-image resolution of 320 x 320 pixels) and once with a binary classification head for each finding, resulting in 210 individual training runs. Overall, training took 340 hours. As to be expected, the training of deeper networks required more time than the training of shallower networks. For an image resolution of 320 x 320 pixels, the training of AlexNet required the least amount of time with a time per epoch of 2:29 to 2:50 minutes and a total duration of 20 minutes for a batch size of 32. Using a smaller batch size of 16, the time per epoch raised to 2:59 - 3:06 minutes and a total duration of 24 minutes. In contrast, using a batch size of 16, training of a DenseNet-201 took the longest with 5:11 hours and epochs requiring 41 minutes. For a batch size of 32, training a DenseNet-169 required the largest amount of time with 3:06 hours (epochs between 21 and 27 minutes). Increasing the batch size from 16 to 32 lead to an average acceleration of training by $29.9\% \pm 9.34\%$. Table 3 gives an overview of training times.

Discussion

In the present work, different architectures of artificial neural networks are analyzed with respect to their performance for the classification of chest radiographs. We could show that more complex neural networks do not necessarily perform better than shallow networks.

Instead, an accurate classification of chest radiographs may be achieved with comparably shallow networks, such as AlexNet (8 layers), ResNet-34 or VGG-16, which surpass even complex deep networks such as ResNet-150 or DenseNet-201.

The use of smaller neural networks has the advantage, that hardware requirements and training time are lower compared to deeper networks. Shorter training times allow to test more hyperparameters, simplifying the overall training process. Lower hardware requirements also enable the use of increased image resolutions. This could be of relevance for the evaluation of chest radiographs with a generic resolution of 2048 x 2048 px to 4280 x 4280 px, where specific findings, such as small pneumothorax, require larger resolutions of input-images, because otherwise the crucial information regarding their presence could be lost due to a downscaling. Furthermore, shorter training times might simplify the integration of improvement methods into the training data, such as the implementation of ‘human in the loop’ annotations. ‘Human in the loop’ implies that the training of a network is supervised by a human expert, who may intervene and correct the network at critical steps. For example, the human expert can check the misclassifications with the highest loss for incorrect labels, thus effectively reducing label noise. With shorter training times, such feedback loops can be executed faster. In the CheXpert dataset, which was used as a groundwork for the present analysis, labels for the images were generated using a specifically developed natural language processing tool, which did not produce perfect labels. For example, the F1 scores for the mention and subsequent negation of cardiomegaly were 0.973 and 0.909, and the F1 score for an uncertainty label was 0.727. Therefore, it can be assumed, that there is a certain amount of noise in the training data, which might affect the accuracy of the models trained on it. Implementing a human-in-the loop approach for partially correcting the label noise could further improve performance of networks trained on the CheXpert dataset [8]. Our findings differ from applied techniques used in previous literature, where deeper network architectures, mainly a DenseNet-121, were used instead of small networks to classify the CheXpert data set [11][1][15]. The authors of the CheXpert dataset achieved an average overall AUROC of 0.889 [7], using a DenseNet-121 which was not surpassed by any of the models used in our analysis, although differences between the best performing networks and the CheXpert baseline were smaller than 0.01. It should be noted, however, that in our analysis the hyperparameters for the models were probably not selected as precise as in the original CheXpert paper by Irvin et al., since the focus of this

work was more on comparing the architectures and not on the complete optimization of one specific network. Still, we identified model, which achieved higher AUROC values in two of the five findings (cardiomegaly and effusion). Pham et al. also used a DenseNet-121 as the basis for their model and proposed the most accurate model of the CheXpert dataset with a mean AUROC of 0.940 for the five selected findings [11]. The good results are probably due to the hierarchical structure of the classification framework, which takes into account correlations between different labels, and the application of a label-smoothing technique, which also allows the use of uncertainty labels (which were excluded in our present work). Allaouzi et al. similarly used a DenseNet-121 and created three different models for the classification of the CheXpert and ChestX-ray14, yielding an AUC of 0.72 for atelectasis, 0.87-0.88 for cardiomegaly, 0.74-0.77 for consolidation, 0.86-0.87 for edema and 0.90 for effusion [1]. Except for cardiomegaly, we achieved better values with several models (e.g. ResNet-34, ResNet-50, AlexNet, VGG-16). We would interpret this as proof that complex deep networks are not necessarily superior to more shallow networks for chest x-ray classification. At least for the CheXpert dataset it seems that methods optimizing the handling of uncertainty labels and hierarchical structures of the data are important to improve model performance. Sabottke et al. trained a ResNet-32 for classification of chest radiographs and therefore are one of the few groups using a smaller network [15]. With an AUROC of 0.809 for atelectasis, 0.925 for cardiomegaly, 0.888 for edema and 0.859 for effusion, their network performed not as good as some of our tested networks. Raghu et al. employed a ResNet-50, an Inception-v3 as well as a custom-designed small network. Similar to our findings, they observed, that smaller networks showed a comparable performance to deeper networks [13].

Conclusion

In the present work, we could show that smaller artificial neural networks for the classification of chest radiographs can perform similar, or even surpass deeper and very deep neural networks. In contrast to many previous studies, which mostly used a DenseNet-121, we achieved the best results with up to 95% smaller networks. Using smaller networks therefore has the advantage that they have lower hardware requirements, as they require less GPU RAM and can be trained faster without loss of performance.

Tables

Table 1 Area under the Receiver Operating Characteristic Curve

Network	Batchsize	Atelectasis	Cardiomegaly	Consolidation	Edema	Effusion	Pooled
CheXpert baseline	16	0.818	0.828	0.938	0.934	0.928	0.889
ResNet-18	16	0.816	0.797	0.905	0.868	0.899	0.857
ResNet-34	16	0.799	0.798	0.902	0.891	0.905	0.859
ResNet-50	16	0.798	0.799	0.890	0.880	0.913	0.856
ResNet-101	16	0.813	0.810	0.905	0.889	0.907	0.865
ResNet-152	16	0.801	0.809	0.908	0.896	0.916	0.866
DenseNet-121	16	0.809	0.794	0.895	0.883	0.906	0.857
DenseNet-161	16	0.800	0.817	0.885	0.900	0.923	0.865
DenseNet-169	16	0.805	0.795	0.898	0.891	0.909	0.860
DenseNet-201	16	0.805	0.812	0.891	0.886	0.916	0.862
AlexNet	16	0.790	0.755	0.857	0.894	0.881	0.835
SqueezeNet-1.0	16	0.761	0.755	0.833	0.907	0.885	0.828
SqueezeNet-1.1	16	0.767	0.764	0.880	0.903	0.879	0.839
VGG-13	16	0.798	0.752	0.886	0.867	0.872	0.835
VGG-16	16	0.809	0.766	0.892	0.879	0.883	0.846
VGG-19	16	0.811	0.786	0.901	0.890	0.884	0.854
ResNet-18	32	0.796	0.822	0.908	0.903	0.911	0.868
ResNet-34	32	0.797	0.840	0.903	0.902	0.919	0.872
ResNet-50	32	0.811	0.832	0.916	0.913	0.934	0.881
ResNet-101	32	0.797	0.823	0.911	0.915	0.936	0.876
ResNet-152	32	0.802	0.836	0.917	0.920	0.937	0.882
DenseNet-121	32	0.808	0.828	0.879	0.904	0.926	0.869
DenseNet-161	32	0.809	0.834	0.913	0.923	0.928	0.881
DenseNet-169	32	0.809	0.816	0.900	0.922	0.934	0.876
DenseNet-201	32	0.795	0.820	0.904	0.922	0.931	0.874
AlexNet	32	0.791	0.768	0.856	0.894	0.886	0.839
SqueezeNet-1.0	32	0.773	0.769	0.880	0.913	0.895	0.846
SqueezeNet-1.1	32	0.785	0.789	0.895	0.904	0.898	0.854
VGG-13	32	0.800	0.762	0.883	0.896	0.907	0.850
VGG-16	32	0.798	0.776	0.890	0.911	0.906	0.856
VGG-19	32	0.787	0.790	0.879	0.911	0.916	0.857

Table 1 shows the different areas under the receiver operating characteristic curve (AUROC) for each of the network architectures and individual finding as well as the pooled AUROC per model. According to the pooled AUROC, ResNet-152, ResNet-50 und DenseNet-161 were the best models, while SqueezeNet and AlexNet showed the poorest performance. For cardiomegaly, ResNet-34, ResNet-50, ResNet-152 and DenseNet-161 could surpass the CheXpert baseline provided by Irvin et al. ResNet-50, ResNet-101, ResNet-152 and DenseNet-169 could also surpass the CheXpert baseline for pleural effusion. A batch size of 32 often lead to better results compared to a batch size of 16.

Table 2 Area under the Precision Recall Curve

Network	Batchsize	Atelectasis	Cardiomegaly	Consolidation	Edema	Effusion	Pooled
ResNet-18	16	0.500	0.559	0.806	0.727	0.580	0.634
ResNet-34	16	0.506	0.560	0.804	0.735	0.580	0.637
ResNet-50	16	0.501	0.557	0.802	0.733	0.585	0.636
ResNet-101	16	0.499	0.558	0.765	0.735	0.582	0.628
ResNet-152	16	0.503	0.559	0.808	0.737	0.584	0.638
DenseNet-121	16	0.503	0.554	0.802	0.733	0.580	0.634
DenseNet-161	16	0.501	0.557	0.799	0.736	0.587	0.636
DenseNet-169	16	0.500	0.560	0.805	0.733	0.582	0.636
DenseNet-201	16	0.320	0.555	0.445	0.734	0.582	0.527
AlexNet	16	0.543	0.565	0.490	0.733	0.577	0.582
SqueezeNet-1.0	16	0.509	0.565	0.425	0.736	0.576	0.562
SqueezeNet-1.1	16	0.505	0.563	0.400	0.733	0.575	0.555
VGG-13	16	0.502	0.563	0.761	0.726	0.574	0.625
VGG-16	16	0.501	0.559	0.797	0.733	0.577	0.633
VGG-19	16	0.500	0.558	0.808	0.731	0.577	0.635
ResNet-18	32	0.502	0.557	0.805	0.736	0.582	0.636
ResNet-34	32	0.652	0.556	0.806	0.737	0.585	0.667
ResNet-50	32	0.497	0.555	0.809	0.740	0.590	0.638
ResNet-101	32	0.500	0.558	0.808	0.740	0.591	0.639
ResNet-152	32	0.502	0.559	0.810	0.741	0.591	0.641
DenseNet-121	32	0.500	0.558	0.793	0.736	0.587	0.635
DenseNet-161	32	0.499	0.556	0.808	0.743	0.589	0.639
DenseNet-169	32	0.499	0.556	0.805	0.743	0.588	0.638
DenseNet-201	32	0.502	0.555	0.808	0.742	0.589	0.639
AlexNet	32	0.720	0.562	0.789	0.731	0.578	0.676
SqueezeNet-1.0	32	0.354	0.562	0.815	0.738	0.580	0.610
SqueezeNet-1.1	32	0.506	0.563	0.804	0.731	0.577	0.636
VGG-13	32	0.501	0.560	0.799	0.735	0.578	0.635
VGG-16	32	0.732	0.561	0.804	0.739	0.582	0.684
VGG-19	32	0.501	0.562	0.800	0.740	0.585	0.638

Table 2 shows the area under the precision recall curve (AUPRC) for all networks and findings. In contrast to the AUROC, where deeper models achieved higher values, shallower networks yielded the best results for AUPRC (ResNet-24, AlexNet, VGG-16). DenseNet-201 and Squeezenet showed the lowest AUPRC values. Again, a batch size of 32 appeared to deliver better results compared to a batch size of 16.

Table 3 Duration of Training

Network	Batchsize	Duration/Epoch	Duration/Training
ResNet-18	16	6 min	50 min
ResNet-34	16	10 min	1 h 13 min
ResNet-50	16	11 min - 13 min	1 h 40 min
ResNet-101	16	19 min - 25 min	2 h 47 min
ResNet-152	16	27 min - 28 min	4 h 7 min
SqueezeNet-1.0	16	4 min - 6 min	39 min
SqueezeNet-1.1	16	4 min	37 min
AlexNet	16	3 min	24 min
VGG-13	16	12 min	1 h 49 min
VGG-16	16	20 min - 21 min	2 h 14 min
VGG-19	16	24 min	2 h 40 min
DenseNet-121	16	23 min - 25 min	3 h 7 min
DenseNet-169	16	31 min - 34 min	4 h 21 min
DenseNet-161	16	29 min - 36 min	4 h 17 min
DenseNet-201	16	41 min	5 h 11 min
ResNet-18	32	4 min	31 min
ResNet-34	32	5 min - 7 min	45 min
ResNet-50	32	8 min	1 h 16 min
ResNet-101	32	13 min	2 h 8 min
ResNet-152	32	21 min - 26 min	2 h 58 min
SqueezeNet-1.0	32	3 min - 4 min	28 min
SqueezeNet-1.1	32	3 min	25 min
AlexNet	32	2 min - 3 min	20 min
VGG-13	32	10 min - 14 min	1 h 31 min
VGG-16	32	17 min	1 h 47 min
VGG-19	32	13 min	2 h 2 min
DenseNet-121	32	12 min - 16 min	1 h 49 min
DenseNet-169	32	17 min	2 h 25 min
DenseNet-161	32	21 min - 27 min	3 h 6 min
DenseNet-201	32	20 min	2 h 52 min

Table 3 provides an overview of training time per epoch (duration/epoch) and an overall training-time (duration/training) for each neural network. The times given are the average of five training runs rounded to the nearest minute.

Figures

Receiver Operating Characteristic Curves

Figures 1, 2 and 3 display the ROC-curves for all models. The colored lines represent a single training, black lines represent the pooled performance over five trainings.

Figure 1

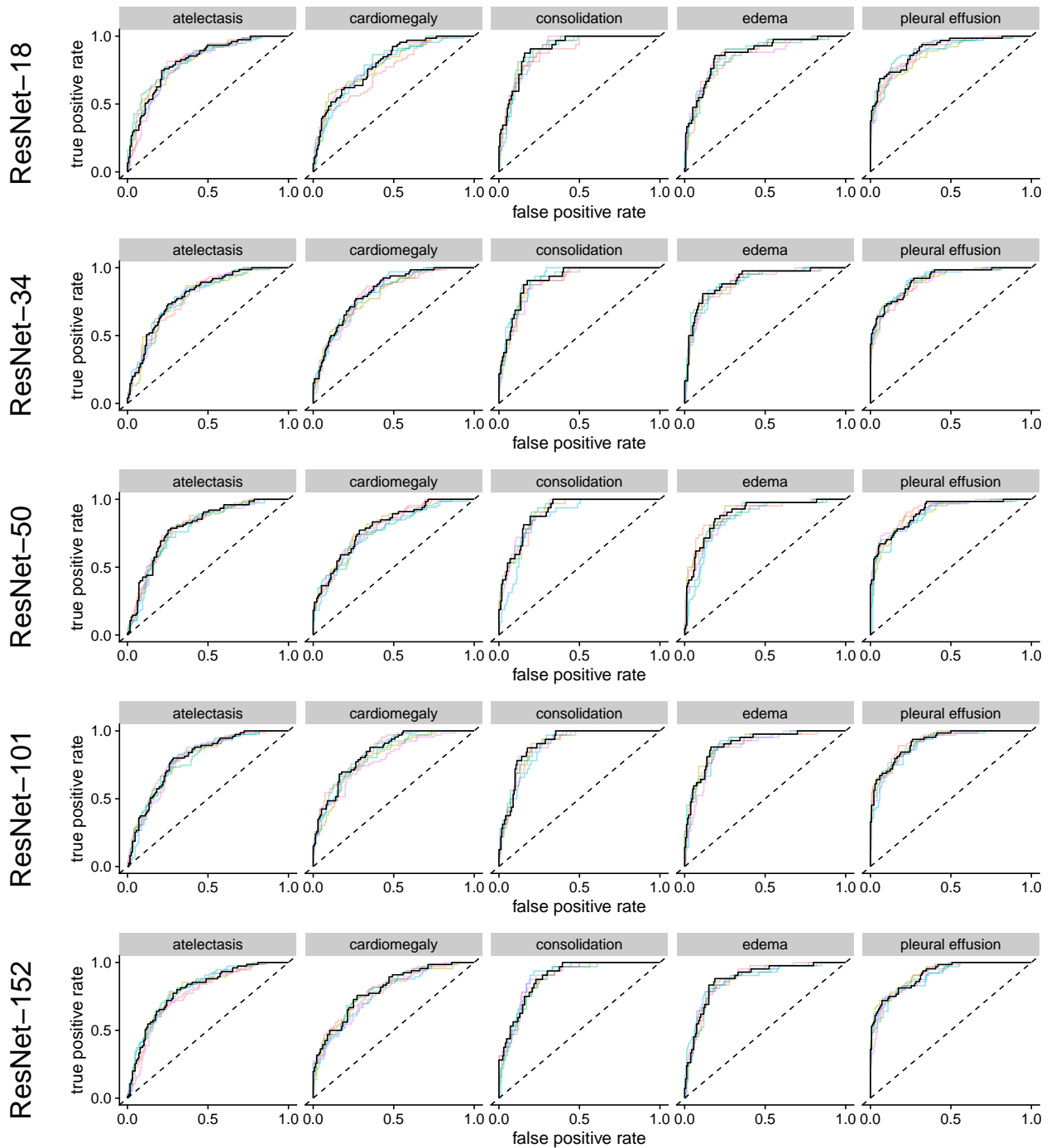


Figure 2

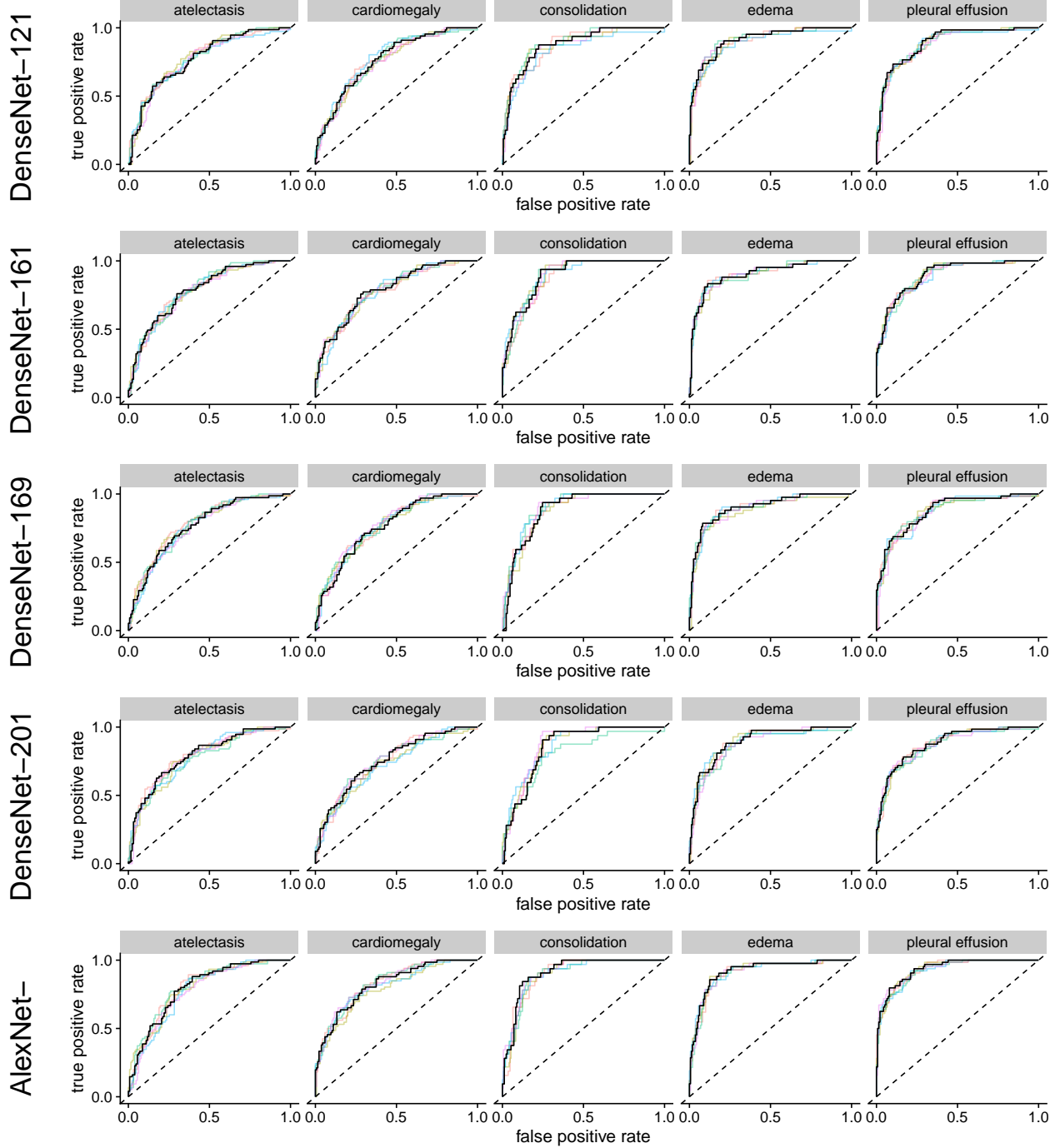
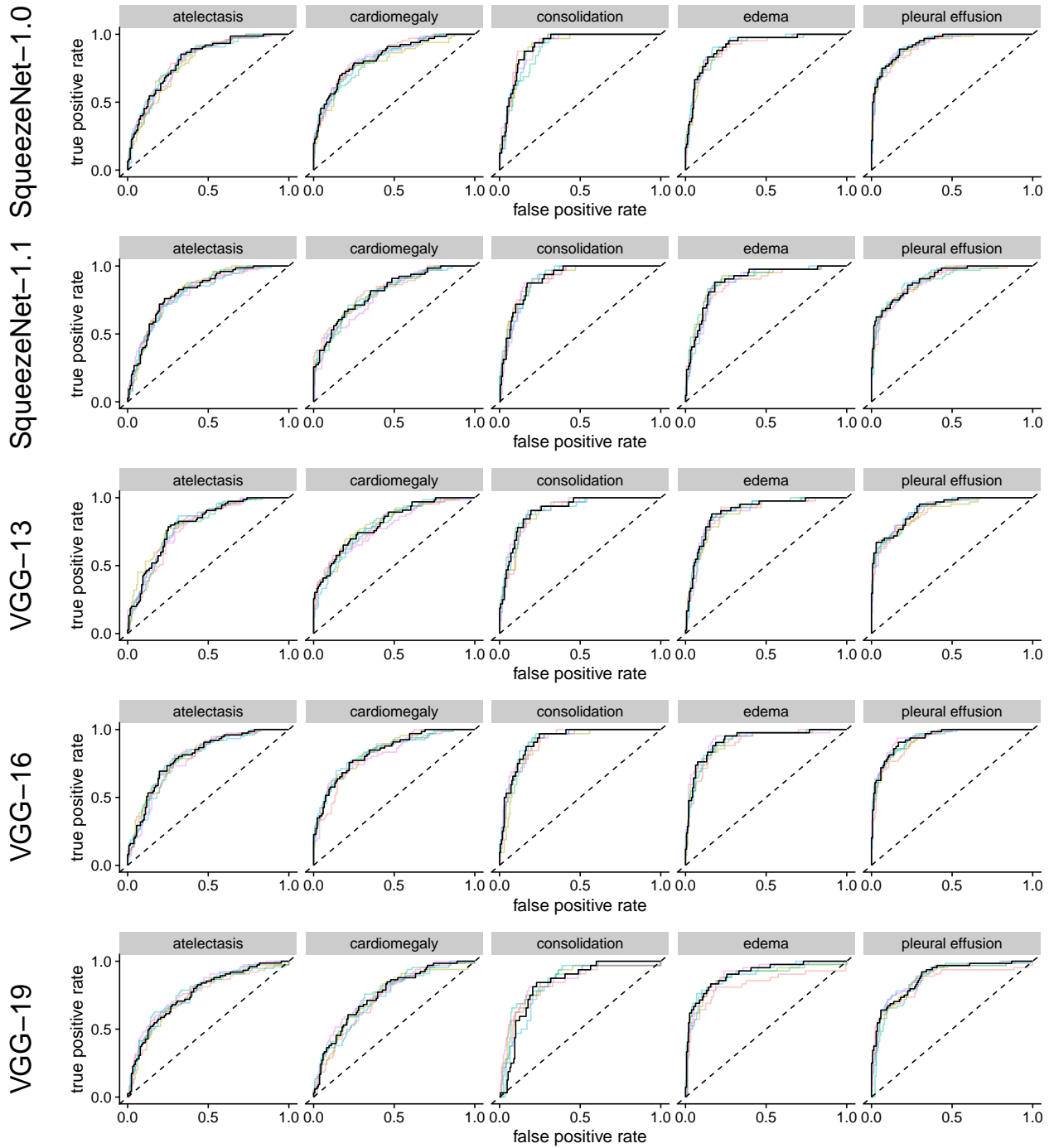


Figure 3



Precision Recall Curves

Figures 1, 2 and 3 display the precision recall curves for all models. The colored lines represent a single training, black lines represent the pooled performance over five trainings.

Figure 4

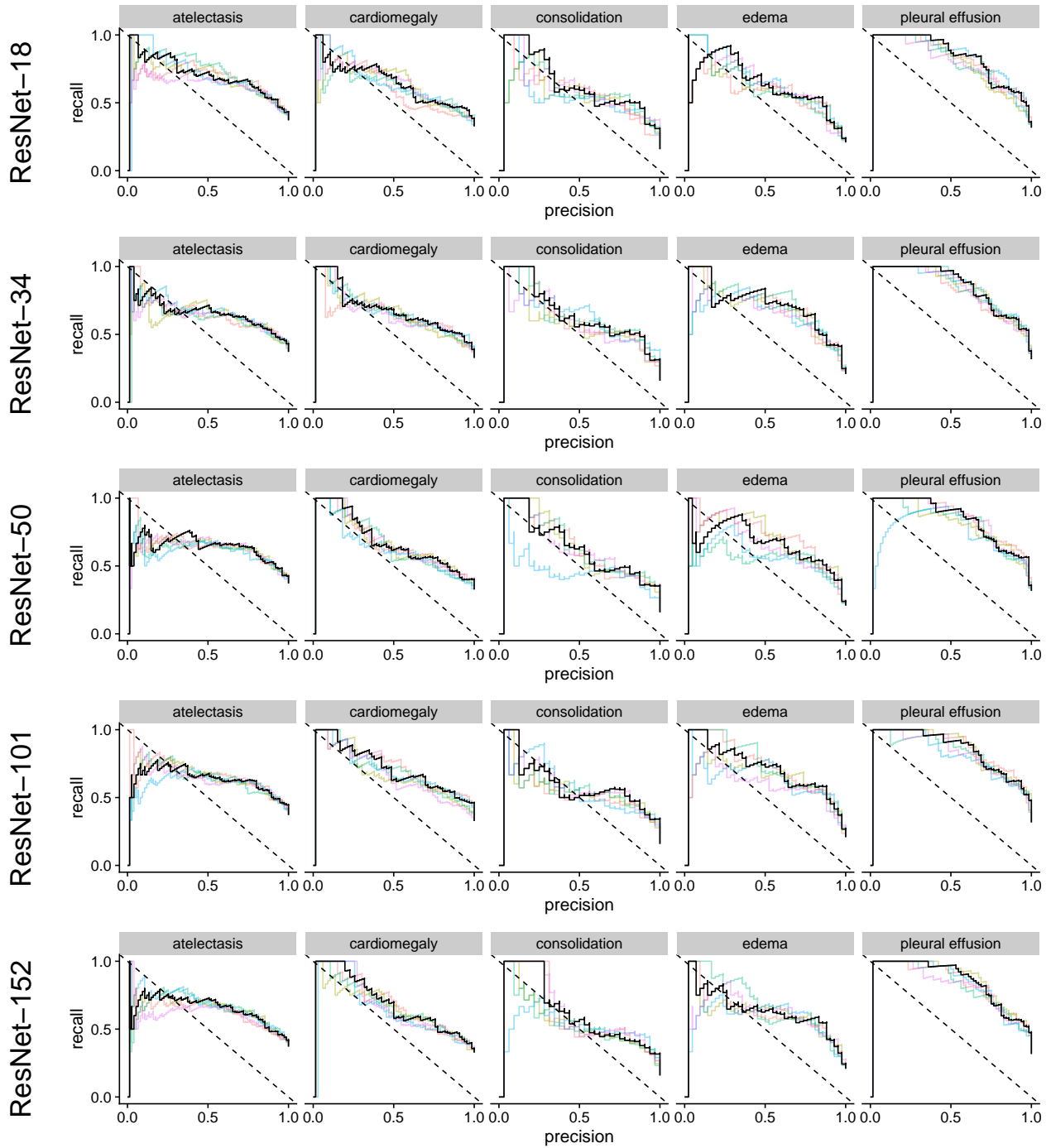


Figure 5

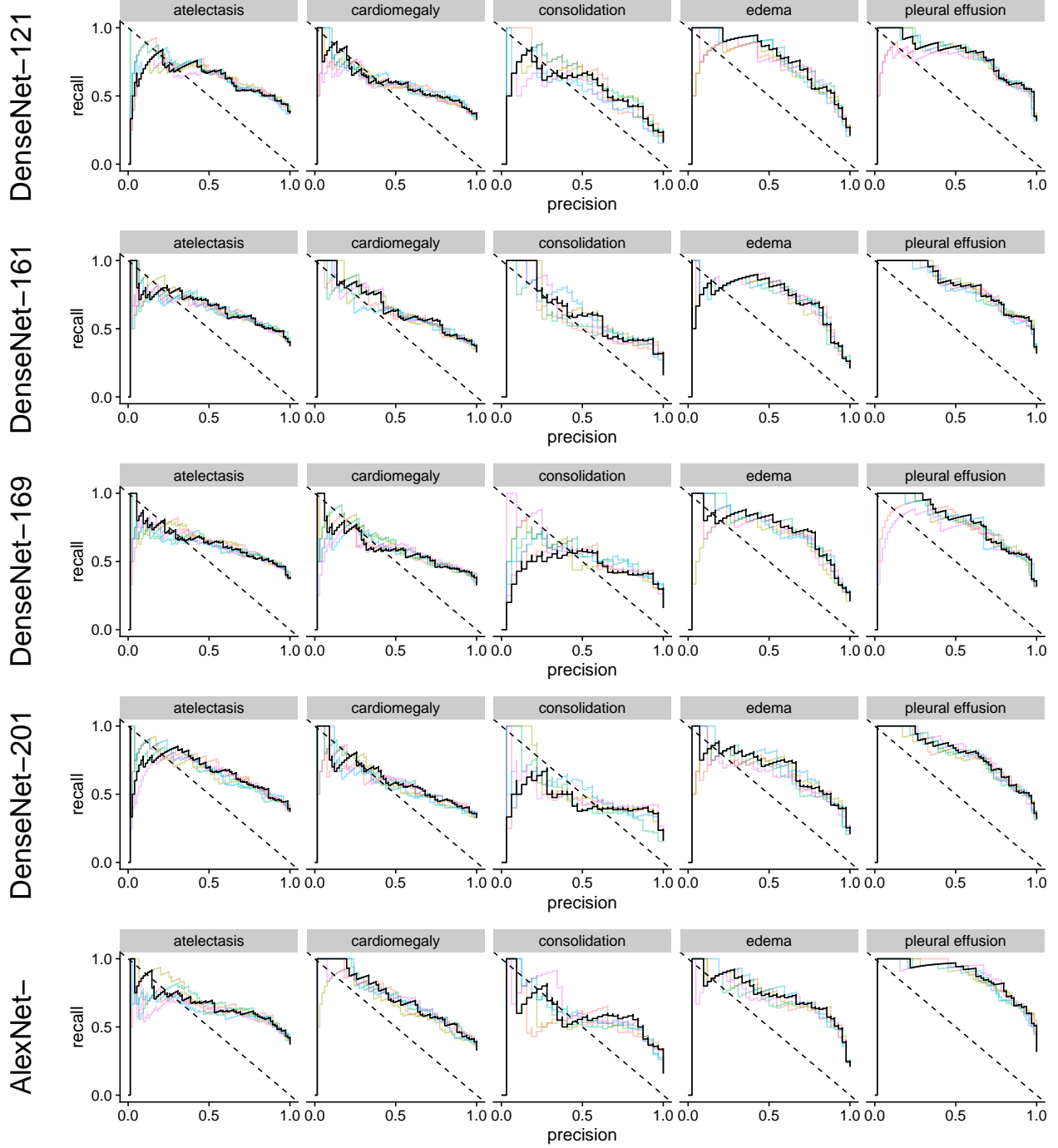
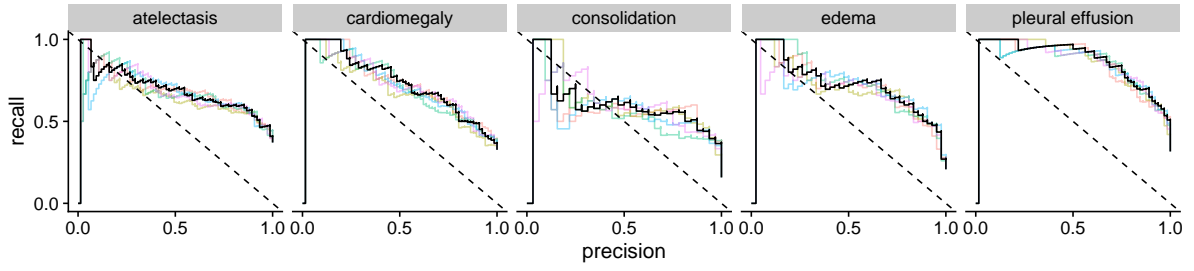
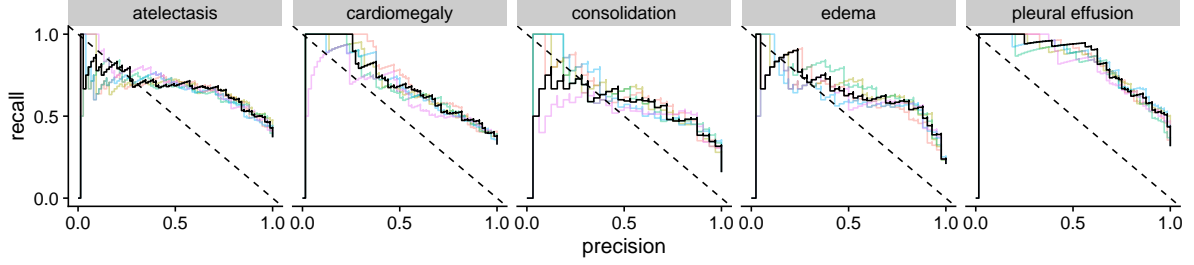


Figure 6

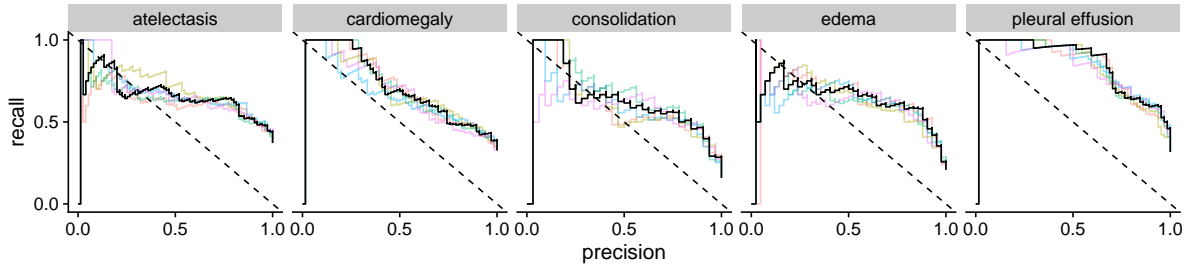
SqueezeNet-1.0



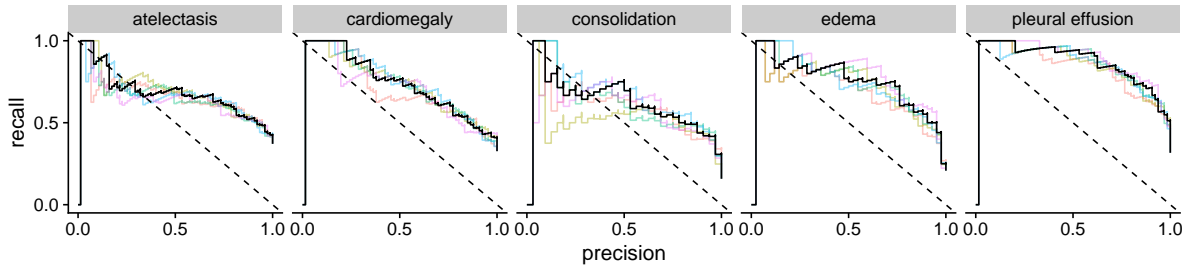
SqueezeNet-1.1



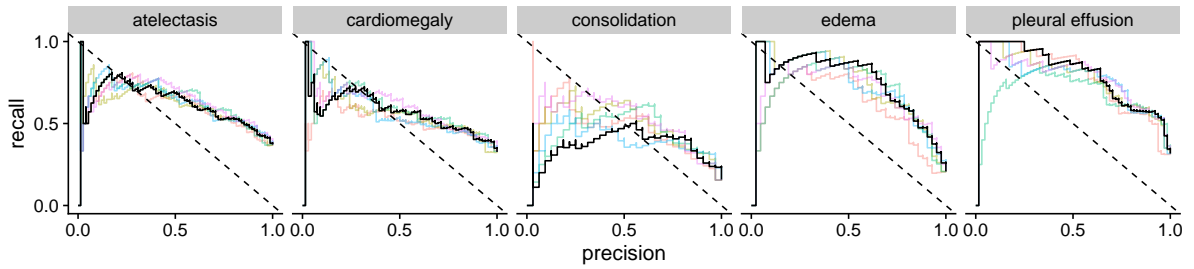
VGG-13



VGG-16



VGG-19



References

- [1] Imane Allaouzi and Mohamed Ben Ahmed. “A novel approach for multi-label chest X-ray classification of common thorax diseases”. In: *IEEE Access* 7 (2019), pp. 64279–64288.
- [2] Aurelia Bustos et al. “Padchest: A large chest x-ray image dataset with multi-label annotated reports”. In: *arXiv preprint arXiv:1901.07441* (2019).
- [3] Kaiming He et al. “Deep residual learning for image recognition”. In: *Proceedings of the IEEE conference on computer vision and pattern recognition*. 2016, pp. 770–778.
- [4] Jeremy Howard et al. *fastai*. <https://github.com/fastai/fastai>. 2018.
- [5] Gao Huang et al. “Densely connected convolutional networks”. In: *Proceedings of the IEEE conference on computer vision and pattern recognition*. 2017, pp. 4700–4708.
- [6] Forrest N Iandola et al. “SqueezeNet: AlexNet-level accuracy with 50x fewer parameters and < 0.5 MB model size”. In: *arXiv preprint arXiv:1602.07360* (2016).
- [7] Jeremy Irvin et al. “Chexpert: A large chest radiograph dataset with uncertainty labels and expert comparison”. In: *Proceedings of the AAAI Conference on Artificial Intelligence*. Vol. 33. 2019, pp. 590–597.
- [8] Davood Karimi et al. “Deep learning with noisy labels: exploring techniques and remedies in medical image analysis”. In: *arXiv preprint arXiv:1912.02911* (2019).
- [9] Alex Krizhevsky, Ilya Sutskever, and Geoffrey E Hinton. “ImageNet Classification with Deep Convolutional Neural Networks”. In: *Advances in Neural Information Processing Systems 25*. Ed. by F. Pereira et al. Curran Associates, Inc., 2012, pp. 1097–1105. URL: <http://papers.nips.cc/paper/4824-imagenet-classification-with-deep-convolutional-neural-networks.pdf>.
- [10] Adam Paszke et al. “PyTorch: An Imperative Style, High-Performance Deep Learning Library”. In: *Advances in Neural Information Processing Systems 32*. Ed. by H. Wallach et al. Curran Associates, Inc., 2019, pp. 8024–8035. URL: <http://papers.neurips.cc/paper/9015-pytorch-an-imperative-style-high-performance-deep-learning-library.pdf>.
- [11] Hieu H Pham et al. “Interpreting chest X-rays via CNNs that exploit disease dependencies and uncertainty labels”. In: *arXiv preprint arXiv:1911.06475* (2019).
- [12] R Core Team. *R: A Language and Environment for Statistical Computing*. R Foundation for Statistical Computing, Vienna, Austria, 2019. URL: <https://www.R-project.org/>.
- [13] Maithra Raghu et al. “Transfusion: Understanding transfer learning for medical imaging”. In: *Advances in Neural Information Processing Systems*. 2019, pp. 3342–3352.
- [14] Pranav Rajpurkar et al. “Chexnet: Radiologist-level pneumonia detection on chest x-rays with deep learning”. In: *arXiv preprint arXiv:1711.05225* (2017).
- [15] Carl F. Sabottke and Bradley M. Spieler. “The Effect of Image Resolution on Deep Learning in Radiography”. In: *Radiology: Artificial Intelligence* 2.1 (2020), e190015. DOI: 10.1148/ryai.2019190015.
- [16] Carl F Sabottke and Bradley M Spieler. “The effect of image resolution on deep learning in radiography”. In: *Radiology: Artificial Intelligence* 2.1 (2020), e190015.
- [17] Karen Simonyan and Andrew Zisserman. “Very deep convolutional networks for large-scale image recognition”. In: *arXiv preprint arXiv:1409.1556* (2014).
- [18] T. Sing et al. “ROCR: visualizing classifier performance in R”. In: *Bioinformatics* 21.20 (2005), p. 7881. URL: <http://rocr.bioinf.mpi-sb.mpg.de>.
- [19] Leslie N Smith. “Cyclical learning rates for training neural networks”. In: *2017 IEEE Winter Conference on Applications of Computer Vision (WACV)*. IEEE. 2017, pp. 464–472.
- [20] Hadley Wickham. *tidyverse: Easily Install and Load the 'Tidyverse'*. R package version 1.2.1. 2017. URL: <https://CRAN.R-project.org/package=tidyverse>.